

B0000024

IRRADIATION TESTING OF MATRIX MATERIAL FOR SPHERICAL HTR-10 FUEL ELEMENTS

**Chunhe Tang /Institute of Nuclear Energy
Technology, Tsinghua University, Beijing
100084, China**

**Yanwen Zou / Institute of Nuclear Energy
Technology, Tsinghua University, Beijing
100084, China**

**Ziqiang Li / Institute of Nuclear Energy
Technology, Tsinghua University, Beijing
100084, China**

ABSTRACT

In order to evaluate if the fuel elements and their components, matrix material and coated fuel particles, can meet the design requirement of 10 MW High Temperature Gas-cooled Reactor, an irradiation test with 4 spherical fuel elements, 60 matrix material specimens of 5mm×5mm×40mm and 13500 coated fuel particles was performed in Russian IVV-2M reactor from July 2000 to February 2003. The irradiation temperature was 1000 . The fast neutron fluence of matrix material specimens reached $1.3 \times 10^{21} \text{cm}^{-2}$ ($E > 0.1 \text{MeV}$). Post irradiation examination contained the visual inspection, dimension measurement and determining the density, porosity, specific electrical resistance and bending strength. The irradiation results are given in this paper, and show that the matrix material for spherical HTR-10 fuel elements made from the domestic raw materials and fabricated by the quasi-isostatic room-temperature moulding process is suitable as a structural material for spherical HTR fuel elements.

1 INTRODUCTION

The 10 MW High Temperature Gas-cooled Reactor (HTR-10) built in China is a modular pebble-bed high temperature gas-cooled reactor. Spherical fuel elements, as shown in Fig.1, are employed in the pebble-bed core [1]. The HTR-10 fuel element with 60 mm in diameter consists of the matrix material (MM) and 8300 coated fuel particles. The LEU (low enriched uranium) TRISO coated fuel particle [2,3] is adopted in the HTR-10 program. The matrix material constitutes the structural material for the spherical fuel elements. It serves as a homogeneous envelopment for the coated fuel particles in a 50 mm diameter inner fuel zone and

a 5 mm thick fuel-free shell enclosing the fuel zone. The coated fuel particle is composed of a central UO_2 kernel of 500 μm in diameter and four layers, which are (1) low density porous pyrolytic carbon (PyC) layer of 95 μm in thickness, (2) an inter high-density isotropic PyC layer with 40 μm in thickness, (3) a SiC layer of 35 μm in thickness, and (4) an outer high-density isotropic PyC layer of 40 μm in thickness. The fabrication technology for HTR-10 fuel element has been established through a lot of R&D activities in the past 20 years in Institute of Nuclear Energy Technology, Tsinghua University (INET)[4,5]. Over 20 000 spherical fuel elements were produced for HTR-10 in 2000 and 2001.

The matrix material is used for the inner and outer zones of spherical HTR-10 fuel elements, and has the same composition as German standard matrix A3-3 [6,7]. It is made from 64 wt% natural graphite powder, 16 wt% petroleum coke graphite powder and 20 wt% phenolic resin binder. The matrix material in fuel elements must have high density to act as a moderator for the fission neutrons, exhibit a good thermal conductivity to perform heat transfer from the coated fuel particle to the surface of the fuel elements, high mechanical strength to resist external forces subjected in the core and the pneumatic transfer of fuel elements, good resistance to corrosion caused by impurities in the coolant gas, and high dimensional stability during the irradiation with fast neutrons.

The domestic natural flake graphite powder, artificial petroleum coke graphite powder and phenolic resin binder were used as the raw materials of the matrix material for spherical HTR-10 fuel elements. The quasi-isostatic room-temperature moulding process was used to produce the fuel elements and fuel-free matrix material spheres from which the specimens for the irradiation test were taken. One of main

objectives of this irradiation test performed in Russian IVV-2M reactor was to evaluate the irradiation behavior of the matrix material fabricated by domestic raw materials and above-mentioned fabrication process.

2 IRRADIATION SPECIMENSE

The quasi-isostatic room-temperature moulding process was used to produce spherical HTR-10 fuel elements. This process consists of the following main steps: 1) The graphitic raw materials are processed to resinated powder by means of mixing, kneading, drying and grinding. 2) For the fabrication of fuel elements the coated fuel particles are overcoated with resinated powder prior to pressing in a rotating drum. The thickness of the resinated powder overcoating layer is Approx. 200 μ m. 3) The fuelled zone of the sphere is premoulded at a low pressure of 4 ~ 5 MPa, and the green fuel sphere is finally moulded at a moulding pressure of 300MPa after the fuelled zone has been embedded in resinated powder for the sphere shell. 4) Lathing to specified size is performed following the moulding. 5) The machined spheres are heated in Ar atmosphere in coking oven for carbonization of the binder in the resinated powder and in vacuum at 1950 in the high temperature furnace to remove the impurities. Figure 2 describes above-mentioned process steps.

The above-mentioned process is also used to produce fuel-free matrix material spheres. Only the process step concerning overcoating the coated fuel particles is omitted.

The irradiated 4 fuel elements were randomly sampled from the first and second product batches. During the production of the first batch of the fuel sphere, the fuel-free graphite spheres, from which the specimens for the irradiation test were taken, were also manufactured. The size of matrix material specimens is 5 mm \times 5mm \times 40mm. The main characteristics of matrix material spheres fabricated are listed in Table 1.

60 matrix material specimens for irradiation testing were cut out of the inner zone of the fuel-free matrix material spheres parallel and perpendicular to the equatorial plane (Fig. 3).

3 IN-PILE IRRADIATION TEST

The irradiation testing was carried out in IVV-2M reactor located in Institute of Nuclear Materials of Russia. The IVV-2M is a pool-type water-cooled and moderated reactor with a thermal power of 15 MW. Its maximum thermal and fast neutron fluxes are $4\times 10^{14}\text{cm}^{-2}\text{s}^{-1}$ and $4\times 10^{14}\text{cm}^{-2}\text{s}^{-1}$, respectively.

The irradiation rig contains 5 independent capsules as shown in Fig. 4a. From top to bottom, these capsules are numbered capsules 1-5. The capsule 1 (Fig. 4b) contains about 13 500 loose coated fuel particles and 60 specimens of matrix material from the graphite spheres. The spherical fuel element SFE5 and SFE7 from the first batch were located in Capsules 2 (Fig. 4c) and 5, respectively, while elements SFE8 and SFE12 from the second batch were located in Capsules 4 and 3.

Each capsule was independently controlled and continuously swept. The irradiation temperature was adjusted by gas mixture ratio of He and Ne in the gap between metal

box and graphite box in the capsule. The heat resource was the fission heat of the coated fuel particle in irradiated specimens and gamma heating.

The irradiation test started in July 2000, and ended up in February 2003. The irradiation temperature was kept at 1000 ± 50 . Their fast neutron fluence reached 1.29×10^{21} , 1.10×10^{21} , 1.31×10^{21} , 1.30×10^{21} and $1.06\times 10^{21}\text{n/cm}^2$ ($E > 0.1\text{MeV}$) for capsule 1 to 5, respectively.

4 POST IRRADIATION EXAMINATION

4.1 VISUAL INSPECTION

Except the SFE8 in Capsule 4 appearances of the irradiated matrix material specimens (Fig. 5a) and spherical fuel element (Fig. 5b) are without any change, and similar to that before the irradiation test under HTR-10 service conditions, any cracks, blisters and corrosive spots are not observed.

A photo of the remnants of the failed element SFE 8 – taken in post-irradiation examination tests – is shown in Fig. 5c. Since the abnormal phenomena were observed [8], the He loop for Capsule 4 was closed after the burnup reached 37,000 MWd/tU (about 5980 effective hours).

The failure reason of Capsule 4 seemed to be a chemical reaction of the matrix material of element SFE8 with ingress impurities through the helium loop, such as oxygen of ingress air. The heat released by this reaction damaged the thermocouple in the fuel-free zone of the fuel element, it damaged also the graphite matrix and the internal metal box as well as the coated fuel particles. This reaction caused the matrix material of element SFE 8 to form a graphite powder agglomerate which proved to be unbreakable during post-irradiation examination conducted in a hot cell.

4.2 DIMENSIONAL MEASUREMENT

The diameters of SFE5, SFE12 and SFE7 perpendicular and parallel to the equatorial plane of the fuel sphere were measured before and after the irradiation test. The measured results are shown in Table 2. At 1000 and the fast neutron fluence of $1.06 \sim 1.31\times 10^{21}\text{cm}^{-2}$ ($E > 0.1\text{MeV}$), the mean shrinkage of irradiated fuel sphere diameters parallel to equatorial plane of the fuel sphere was about 0.66%, while that perpendicular to equatorial plane of the fuel sphere was approx. 0.72%. The results show that the difference of the neutron-induced diameter change perpendicular and parallel to the equatorial plane of the fuel sphere is little.

There are 30 MM specimens perpendicular and parallel to the equatorial plane of the matrix sphere, respectively. Their average lengths before and after the irradiation test are listed in Table 3. As can be seen in this table, the neutron-induced relative length change perpendicular and parallel to the equatorial plane of the matrix sphere is nearly the same. The shrinkages of German graphitic standard matrix A3-3 at 920 and 1120 and $1.3\times 10^{21}\text{cm}^{-2}$ were 0.5% and 0.8%, respectively (No data were available for 1000 [5]). Like A3-3, the matrix material for HTR-10 fuel is dimensionally most

stable at 1000 and $1.3 \times 10^{21} \text{cm}^{-2}$ (HTR-10 service conditions).

The difference of neutron-induced dimensional change in parallel and perpendicular to the equatorial plane for both spherical fuel element and the specimens of the graphite sphere is not obvious. It shows the matrix material for HTR-10 fuel sphere is isotropic.

A comparison between Tables 2 and 3 shows the fuel elements shrank slightly more than the specimens from graphite sphere at the nearly same irradiation temperature and fast neutron fluence. It may be the influence of the size of irradiated specimen on the dimension change. Morgan [9] and Nightingale [10] obtained also the similar results that the shrinkage of large graphite specimen is more than that of small at the same irradiation conditions.

4.3 DETERMINATION OF DENSITY AND POROSITY

The measurements of the density and porosity of MM specimens were carried out by the standard method of hydrostatic weighing in kerosene. The weighing in air and kerosene was carried out by analytical balance. Before weighing in air the samples were dried for 2 hours to remove moisture in exhaust hood. The filling of the open pores of the samples with kerosene was performed by merging the sample into a basin with kerosene in a exsiccator after reaching vacuum.

MM geometrical density ρ , the density without open pores ρ_{no} , the ratio of open pores R_o and ratio of closed pores R_c can be calculated by the following formulas[11]:

MM apparent density:

$$\rho_{MM} = m_a \cdot \rho_k / (\rho_k \cdot m_k), \quad \dots (1)$$

where m_a - mass of sample in air, g;
 ρ_k - density of kerosene, g/cm^3 ;
 m_f - mass of sample, in which open pores are filled in by kerosene, in air, g;
 m_k - mass of sample in which open pores are filled in by kerosene, in kerosene, g.

MM density without open pores:

$$\rho_{no} = m_a \cdot \rho_k / (m_a - m_k). \quad \dots (2)$$

Ratio of open pores:

$$R_o = (m_f - m_a) / (m_f - m_k) \cdot 100\%. \quad \dots (3)$$

Ratio of closed pores:

$$R_c = (\rho_t - \rho_{no}) / \rho_t \cdot 100\%, \quad \dots (4)$$

where ρ_t - theoretical density of graphite.

The apparent density, density without open pores, open and closed porosity of 10 specimens parallel to the equatorial plane and 10 specimens perpendicular to the equatorial plane were measured before and after the irradiation testing. Their measurement results are listed in Table 4.

As can be seen in Table 4, the irradiation induced increase of both geometrical density and density without open pores. It also shows that the irradiation caused the shrinkage of the matrix material. Table 4 also gives the increase of the neutron-induced ratio of open pores and the decrease of the neutron-induced ratio of closed pores. This result shows some closed pores may be transformed into open pores due to neutron-induced shrinkage of matrix material and irradiation-induced defects of lattice in the matrix material.

Delle etc investigation [10] proved that the total porosity of the matrix material is decreased by irradiation because the graphite crystallites expand into the micropores and the macropores serve as a buffer volume for the dimensional changes within the bulk material, and that the open porosity of the matrix material is increased by fast neutron exposure. Our measurement results are consistent with their finding.

4.4 DETERMINATION OF SPECIFIC ELECTRICAL RESISTANCE

Though the specific electrical resistance is not very important for matrix material, the studies of the effects of fast neutron irradiation have been very extensively performed because they supply important clues concerning the extent of crystal-lattice damage, and the specific electrical resistance is closely related to thermal conductivity and is easy to measure.

The specific electrical resistance (r) of the matrix material specimens with a constant cross section is:

$$r = R \cdot S / L, \quad \dots (5)$$

where S — cross section area of specimen, m^2 ;
 L — length between two points of potential measurement, m;
 R — electrical resistance in length L , Ω .

$$R = U_0 / I_0, \quad \dots (6)$$

where U_0 — the potential difference in L length, V;
 I_0 — the current through the specimen, A.

Before and after the irradiation testing, the electrical resistances of 3 specimens parallel to the equatorial plane and of 3 specimens perpendicular to the equatorial plane were measured from room temperature to 1000 . There was no any difference for specific electrical resistance between parallel and perpendicular to the equatorial plane at the same measurement temperature. However, the irradiation induced the increase of the specific electrical resistance (see Fig.6). At room temperature, the increase of the specific electrical resistance induced by irradiation was 48%, at 1000 , 19%.

The electric conductivity of the matrix material of the fuel sphere depends on the scattering of the phonon and electron in the crystal boundary. Collision of a fast neutron with a carbon atom produces a high energy "knock on" carbon atom which creates interstitial and vacancy defects, in which electrons are scattered. Therefore, the fast neutron irradiation induced increase of the specific electrical resistance of matrix material.

4.5 MEASUREMENT OF BENDING STRENGTH

The bending strength (σ_b) of specimens was measured by three-point bending method, and calculated by the following formula:

$$\sigma_b = 3P \cdot L / 2b \cdot h^2, \quad \dots (7)$$

where P — breaking load, kN;
 L — distance between the support points, mm;
 b — specimen width, mm;
 h — specimen height, mm.

The specimens of $5\text{mm} \times 5\text{mm} \times 40\text{mm}$ were used for the measurement of the bending strength. In parallel to the equatorial plane, 16 specimens before irradiation and 12

specimens after irradiation were determined, respectively. Their average bending strengths are 26.0 MPa and 27.8 MPa, respectively. The increase of the bending strength induced by irradiation is 6.9%. In perpendicular to the equatorial plane, 15 specimens before irradiation and 12 specimens after irradiation were determined, respectively. Their average bending strengths are 24.1 MPa and 28.0 MPa, respectively. The increase of bending strength induced by irradiation is 16.2%.

As a result of a large number of interstitials and vacancies (Frenkel defects) in the post-irradiation matrix material induced by fast neutron bombardment, the neutron irradiation induces the increase of the bending strength of the matrix material. These effects of irradiation on the bending strength are similar to those on the strength of other materials.

5 CONCLUSION

Under HTR-10 service conditions (the fuel element temperature: 1000 and fast neutron fluence: $\sim 1.0 \times 10^{21} \text{cm}^{-2}$), the main irradiation results of MM for spherical HTR-10 fuel elements made from the domestic raw materials and fabricated by the quasi-isostatic room-temperature moulding process are as follows:

- 1) The average shrinkages of the length of MM specimens and spherical fuel elements were $\sim 0.3\%$ and $\sim 0.7\%$, respectively. The difference of the shrinkage between MM specimens and fuel spheres may be the influence of the size of irradiated specimen on the dimension change. The difference of neutron-induced dimensional change in parallel and perpendicular to the equatorial plane for both spherical fuel element and the specimens of the graphite sphere is not obvious.
- 2) The results of the density measurement show that the irradiation caused the increase of the geometrical density, density without open pores, and the ratio of open pores, and the decrease of the ratio of closed pores.
- 3) The irradiation induced the increase of the specific electrical resistance (see Fig.5). At room temperature, the increase of the specific electrical resistance induced by irradiation was 48%, at 1000 , 19%.
- 4) The irradiation-induced increases of the bending strength of the MM specimens parallel and perpendicular to the equatorial plane were 6.9% and 16.25, respectively.

ACKNOWLEDGMENTS

The reported researches were performed within framework of the project "10MW High Temperature Gas-cooled Reactor" in the Energy Technology Area of the National 863 Programme. The sample inspections before and after the irradiation testing were carried out in Russian Research Center "Kurchatov Institute", Moscow, Russia. The irradiation testing was performed in Institute of Nuclear Materials, Zarechny, Sverdlovsk Region, Russia. The authors appreciate Mr. Oleg G. Karlov, Mr. Yu.G. Degaltsev and Mr.

Vladimir I. Vasiliev for the coordination of the irradiation testing project and for the sample inspections, and also acknowledge Mr. Konstantin, Mr. N. Koshcheyev and Mr. Alexandre V. Kozlov for performing the irradiation testing.

REFERENCES

- [1] Xu, Y.H., Qin, Z.Y., and Wu, Z.X., 1994, "Design of the 10 MW High Temperature Gas-Cooled Reactor," *Journal of Tsinghua University*, **34**(ES2), pp. 10-15.
- [2] Stansfield, O.M., 1991, "Evolution of HTGR Coated Particle Fuel Design," *Energy*, **16** (1/2), pp. 33-45.
- [3] Nabielek, H., Kuehnein, w., and Schenk, w., 1990, "Development of Advanced HTR Fuel Elements," *Nuclear Engineering and Design*, **121**, pp. 199-210.
- [4] Tang, C.H. , Tang, Y.P., Zhu, J.G., Qiu, X.L., Li, J.H., and Xu, S.J., 2000, "Research and Development of Fuel Element for Chinese 10 MW High Temperature Gas-cooled Reactor," *J. of Nucl. Sci. and Technol.* **37** (9), pp. 802-806.
- [5] Tang, C.H., Tang, Y.P., Zhu, J.G., Zou, Y.W., Li, J.H., and Ni, X.J., 2002, "Design and Manufacture of the Fuel Element for the 10 MW High Temperature Gas-cooled Reactor," *Nuclear Engineering and Design*, **218**, pp. 91-102.
- [6] Schulze, R. E., Schulze H.A., and Rind, W., 1982, "Graphite Matrix Materials for Spherical HTR Fuel Elements," *Technical Report No. Juel-Spez-167*, Kernforschungsanlage Juelich GmbH, Juelich.
- [7] Hrovat, M., Nickel, H., and Koizlik, K., 1973, "Ueber die Entwicklung eines Matrixmaterials zur Herstellung gepresster Brennelemente fuer Hoch temperatur-Reaktoren," *Technical Report No. Juel-969-RW*, Kernforschungsanlage Juelich GmbH, Juelich.
- [8] Degaltsev, Yu.G., Grebennik, V.N., Safonov, V.A., et al., 2003, "Report of irradiation to burnup value 100 000 MWd/T(U)," *RRC KI and SF NIKIET*.
- [9] Morgan, W.C., 1964, "Effect of Low Compressive Stresses on Radiation-induced Dimensional Change in Graphite," *Carbon*, **1**(3), pp. 255-257.
- [10] Nightingale, R., and Woodruff, E., 1964, "Radiation Induced Dimensional Changes in Large Graphite Bars," *Nuclear Science Engineering*, **19**(4), pp. 390-395.
- [11] Degaltsev, Y.G., Karlov, O.G., Safonov, V.A., Sinelnikov, L.P., and Koshcheyev, K.N., 2004, "Final Report of Irradiation Testing of the VOSTOK-K for HTR-10 Spherical Fuel Elements, Coated Fuel Particles and Matrix material," *RRC KI and SF NIKIET*.
- [12] Delle, W., Koizlik, K., and Nickel, H., 1983, *Graphitische Werkstoffe Fuer den Einsatz in Kernreaktoren*, Karl Thiemig AG, Muenchen, pp. 121-122, Chap. 4.

ANNEX A

FIGURE CAPTIONS

Fig.1 HTR-10 spherical fuel element

Fig.2 Schematic diagram of manufacturing the fuel and fuel-free spheres

Fig.3 Irradiation specimens cut out of MM sphere parallel and perpendicular to the equatorial plane

Fig.4 Irradiation Facilities

a. Irradiation rig b. Capsule 1 c. One of capsules from 2 to 5

Fig.5 Photographs of the irradiated matrix material specimens and spherical fuel elements

a: Matrix material specimens b: SFE12 c: SFE 8 in Capsule 4 taken in post-irradiation examination

Fig.6 Irradiation-induced specific electrical resistance change of MM specimens

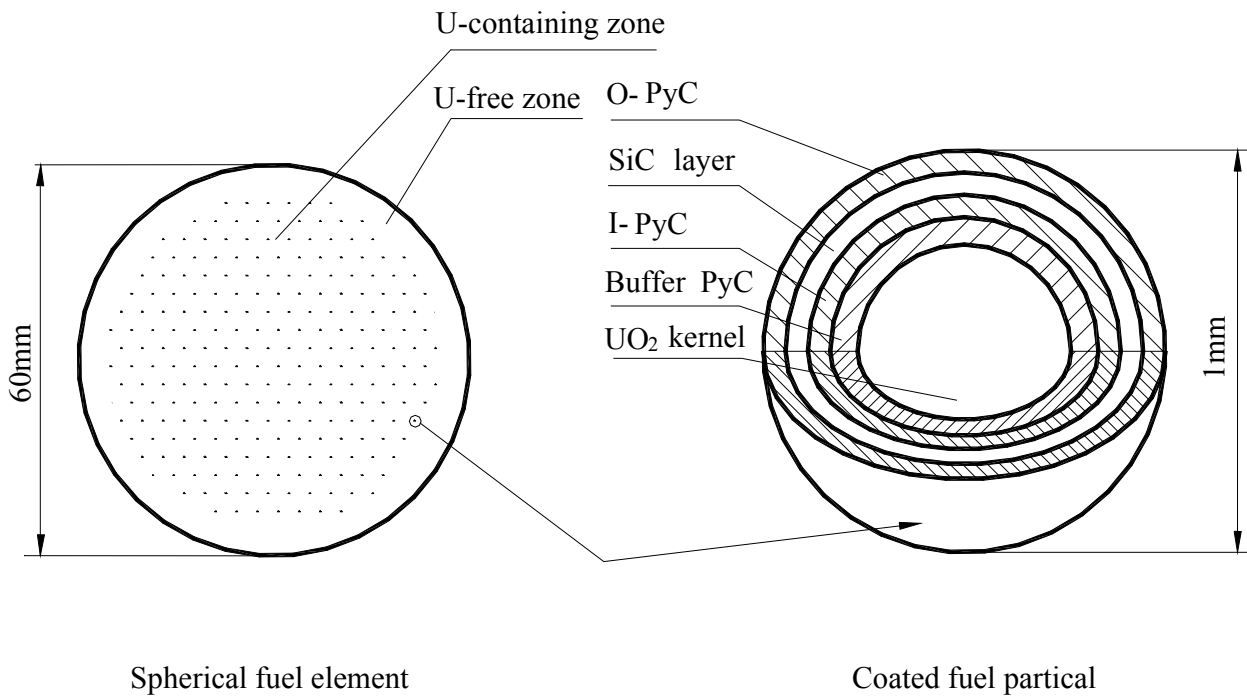


Fig . 1 . HTR-10 spherical fuel element

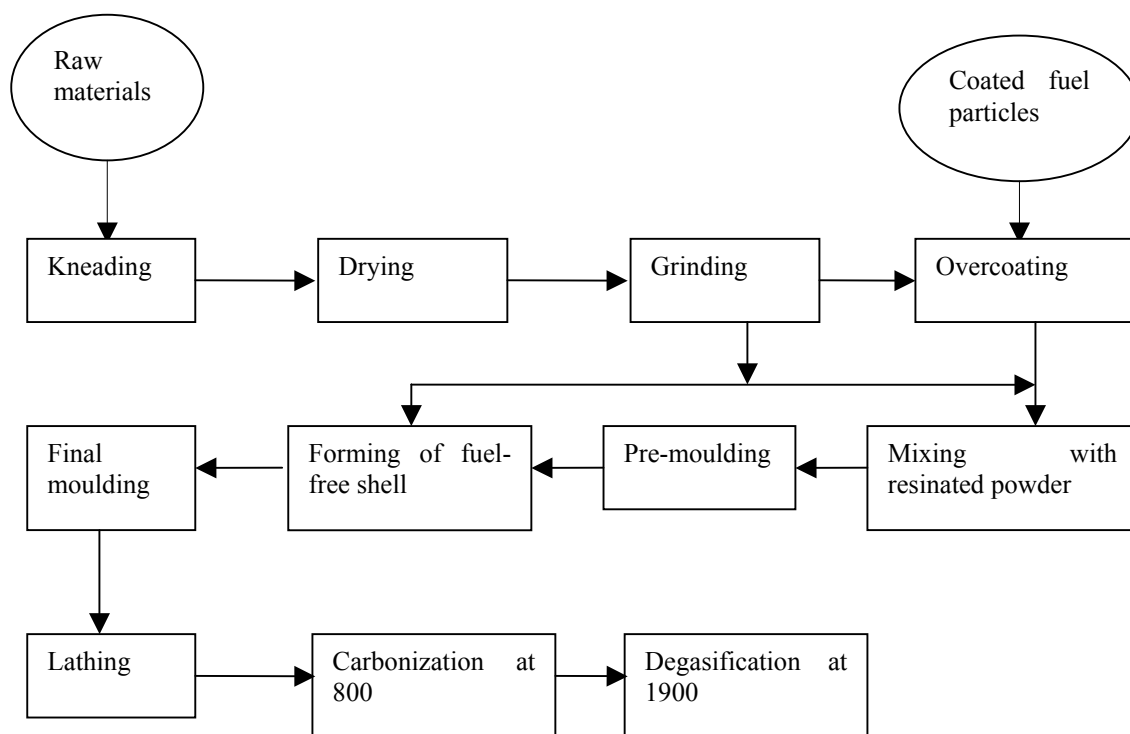


Fig.2 Schematic diagram of manufacturing the fuel and fuel-free spheres

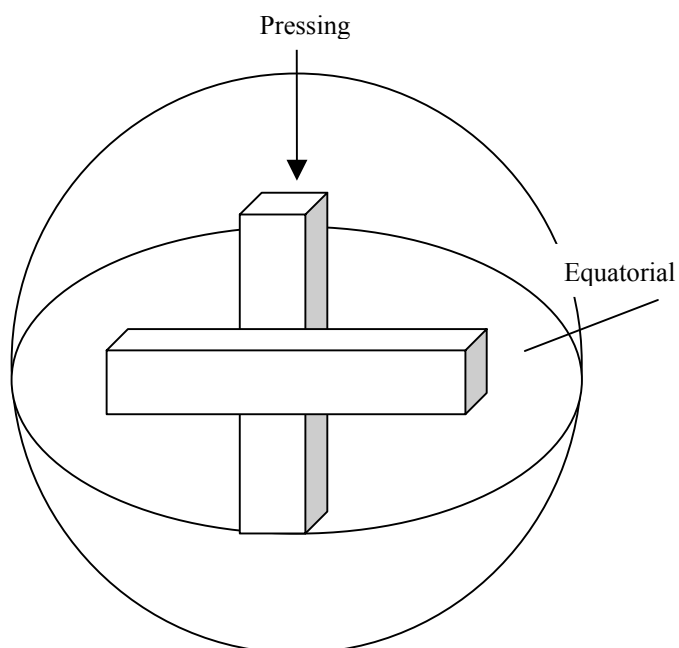


Fig.3 Irradiation specimens cut out of MM sphere parallel and perpendicular to the equatorial plane

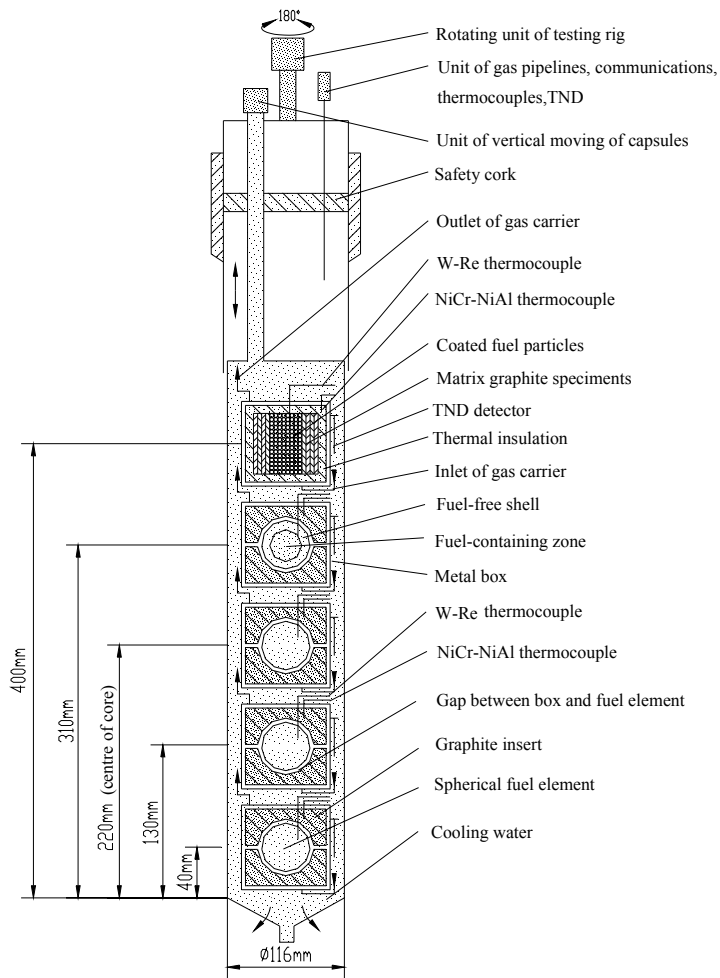


Fig. 4a

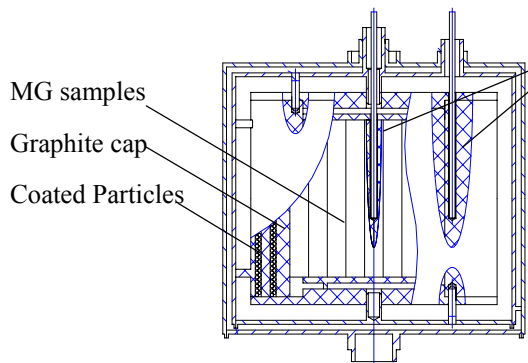


Fig. 4b

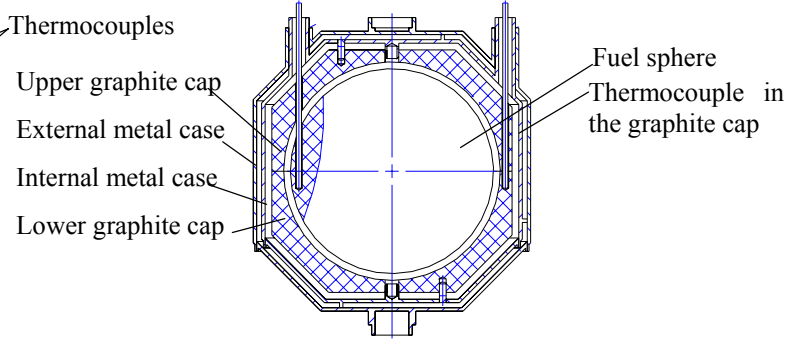


Fig. 4c

Fig.4 Irradiation facilities

- a. Irradiation rig b. Capsule 1 c. One of capsules from 2 to 5



Fig. 5a

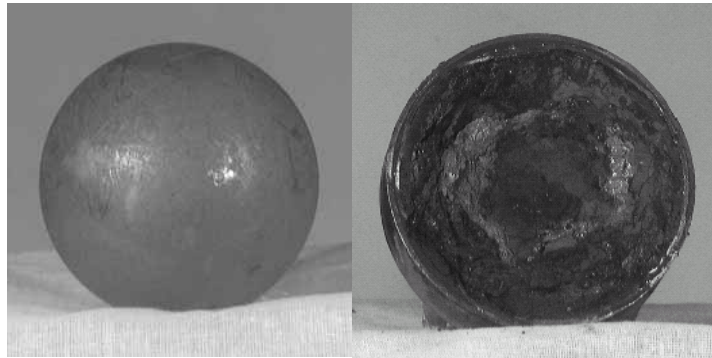


Fig. 5b

Fig. 5c

Fig.5 Photographs of the irradiated matrix material specimens and spherical fuel elements
 a. Matrix material specimens b. SFE12 c. SFE 8 in Capsule 4 taken in post-irradiation examination

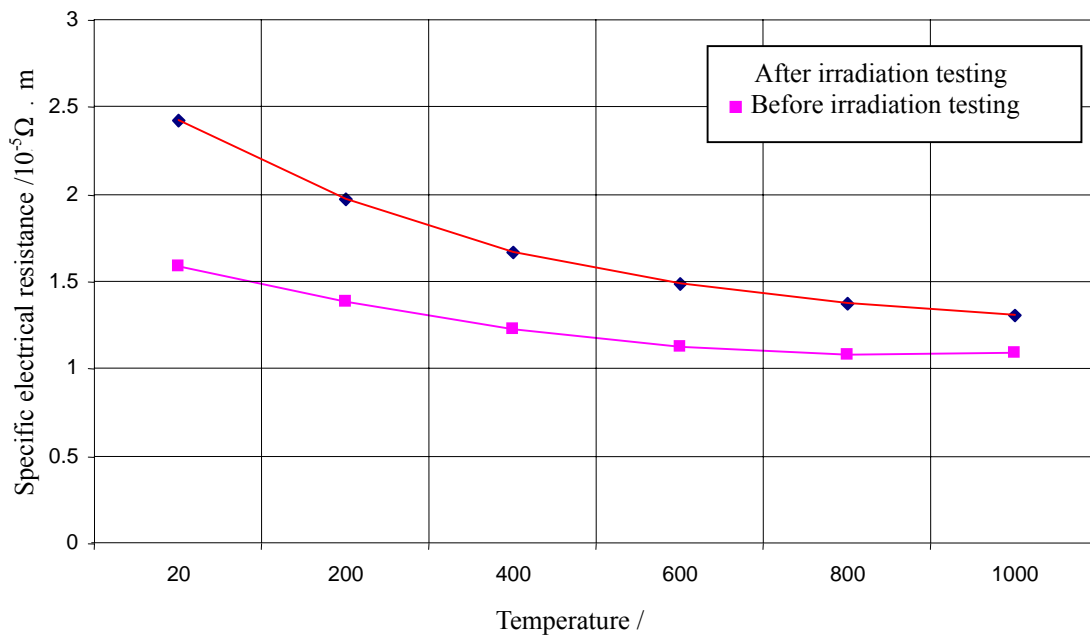


Fig.5 Irradiation-induced specific electrical resistance change of MM specimens

ANNEX B

TABLE CAPTIONS

Table 1

Main characteristics of matrix material spheres

Table 2

Neutron-induced diameter change of the fuel elements at 1000

Table 3

Neutron-induced average length change of matrix material specimens at 1000

Table 4

Neutron-induced density and porosity change of MM specimens at 1000

Table 1

Main characteristics of matrix material spheres

| Characteristics | Value |
|---|--------------|
| Geometrical density $/(g/cm^3)$ | 1.73 |
| Total ash $/(μg/g)$ | 91 |
| Li content $/(μg/g)$ | <0.01 |
| B equivalent $/(μg/g)$ | 1.14 |
| Corrosion rate at 1000 , in He of 1 bar with 1 vol.%%H ₂ O (10h) $/(MM/cm^2·h)$ | 1.0 |
| Erosion rate $/(μg/ball·h)$ | 3.0 |
| Falling strength (fall of a test sphere from a height of 4 m onto sphere bed)/(Number of falls till fracture) | 449 |
| Breaking loading $/(kN)$ | 25.1 22.9 |
| Thermal conductivity at 1000 $/(W/cm·K)$ | 29.3 29.7 |
| Coefficient of linear thermal expansion $(20-500)/10^{-6}K^{-1}$ | 2.72 2.99 |
| Quotient of coefficient of thermal expansion $/(α /α)$ | 1.10 |

Table 2

Neutron-induced diameter change of the fuel elements at 1000

| Fuel element | Fast neutron Fluence (E > 0.1MeV) $/(10^{21}cm^{-2})$ | Before irradiation $/(mm)$ | After irradiation $/(mm)$ | Relative change $/(%)$ | |
|--|---|----------------------------|---------------------------|------------------------|-------|
| Parallel to equatorial plane of fuel sphere | SFE5 | 1.10 | 60.03 | 59.62 | -0.68 |
| | SFE12 | 1.31 | 60.04 | 59.67 | -0.62 |
| | SFE7 | 1.06 | 60.06 | 59.66 | -0.67 |
| Perpendicular to equatorial plane of fuel sphere | SFE5 | 1.10 | 59.90 | 59.48 | -0.70 |
| | SFE12 | 1.31 | 60.06 | 59.62 | -0.73 |
| | SFE7 | 1.06 | 60.10 | 59.67 | -0.72 |

Table 3

Neutron-induced average length change of matrix material specimens at 1000

| Matrix material | Average length before irradiation /(mm) | Average length at $3 \times 10^{21} \text{cm}^{-2}$ ($E > 0.1 \text{MeV}$)/(mm) | Relative change /(%) |
|---|--|---|----------------------|
| 30 specimens parallel to equatorial plane of matrix sphere | 40.02 | 39.90 | -0.30 |
| 30 specimens perpendicular to equatorial plane of matrix sphere | 39.82 | 39.69 | -0.33 |

Table 4

Neutron-induced density and porosity change of MM specimens at 1000

| Matrix material | | Before irradiation | After $1.3 \times 10^{21} \text{cm}^{-2}$ irradiation | Relative change /(%) |
|--|--|--------------------|---|----------------------|
| Average density /(g/cm^3) | 10 specimens perpendicular to the equatorial plane | 1.722 | 1.740 | 1.05 |
| | 10 specimens parallel to the equatorial plane | 1.725 | 1.739 | 0.81 |
| Average density without open pores /(g/cm^3) | 10 specimens perpendicular to the equatorial plane | 1.929 | 1.936 | 0.36 |
| | 10 specimens parallel to the equatorial plane | 1.928 | 1.965 | 1.92 |
| Ratio of open pores /(%) | 10 specimens perpendicular to the equatorial plane | 10.77 | 11.00 | 2.13 |
| | 10 specimens parallel to the equatorial plane | 10.22 | 11.54 | 12.92 |
| Ratio of close pores /(%) | 10 specimens perpendicular to the equatorial plane | 13.88 | 12.90 | -7.06 |
| | 10 specimens parallel to the equatorial plane | 14.21 | 12.29 | -13.51 |